LASER INTERFEROMETER GRAVITATIONAL WAVE OBSERVATORY
- LIGO -
CALIFORNIA INSTITUTE OF TECHNOLOGY
MASSACHUSETTS INSTITUTE OF TECHNOLOGY

Technical Note **LIGO-T2500249v1-G** 07/30/2025

2025 LIGO SURF Final Report: Numerical Simulation of Quantum Enhanced Interferometer Readout

Reilly Loughman
Hamilton College

California Institute of Technology
LIGO Project, MS 18-34
Pasadena, CA 91125
Phone (626) 395-2129
Fax (626) 304-9834
E-mail: info@ligo.caltech.edu

Massachusetts Institute of Technology
LIGO Project, Room NW17-161
Cambridge, MA 02139
Phone (617) 253-4824
Fax (617) 253-7014
E-mail: info@ligo.mit.edu

LIGO Hanford Observatory
Route 10, Mile Marker 2
Richland, WA 99352
Phone (509) 372-8106
Fax (509) 372-8137
E-mail: info@ligo.caltech.edu

LIGO Livingston Observatory
19100 LIGO Lane
Livingston, LA 70754
Phone (225) 686-3100
Fax (225) 686-7189
E-mail: info@ligo.caltech.edu

http://www.ligo.caltech.edu/

1 Abstract

The Rubidium Quantum sensing (RbQ) experiment uses a quantum enhanced measurement system to increase the sensitivity of the GQuEST experiment, which aims to detect quantum gravitational effects through phase shifts in a tabletop interferometer. To support the development of RBQ, I constructed quantum-optical simulations to explore atom-light interactions in cavity systems. The simulation framework investigates how control pulse timing, frequency, and amplitude affect signal detection, and calculates the Quantum Fisher Information (QFI) to identify which experimental parameters, such as cavity loss or coupling strength, most impact sensitivity. An application is a Λ-type rubidium atom transition between three hyperfine states, where a signal and control field drive the two legs of the transition. By fixing the signal, the control can be optimized to maximize energy transfer between the ground states. These results inform the design of RbQ and provide a foundation for optimizing quantum sensing in future gravitational wave detectors, where simulation-driven tuning can improve precision and mitigate the effects of noise.

2 Introduction

Despite its central role in our description of the universe, gravity is unique among the fundamental forces in that we still do not have a consistent quantum description of it. General relativity and quantum mechanics are both extremely successful in their own domains, but combining them into a single framework remains one of the biggest unsolved problems in physics. A working theory of quantum gravity could shed light on what spacetime looks like at the smallest scales, on how the universe began, and on the fate of information in black holes. At present, though, gravity is only understood as an effective field theory at low energies and there has been no direct experimental evidence of any signatures of gravity's true quantum nature.

The holographic principle provides one of the most compelling clues towards such a theory. This idea suggests that the degrees of freedom in a region of space scale with its surface area, not its volume. Building on this, Erik Verlinde and Kathryn Zurek[1] proposed that spacetime itself could be made up of correlated Plank-scale "pixels". And because all quantum systems are subject to fluctuations from uncertainty, these microscopic spacetime degrees of freedom would not remain fixed but instead jitter randomly. If gravity is quantum, then measurable distances themselves must fluctuated in a correlated way, producing what are known as geontropic fluctuations. These fluctuations would act like tiny random phase shifts on light as it propagates, and in principle, they could be picked up by a sufficiently sensitive interferometer.

Modern interferometers such as LIGO already operate close to the fundamental quantum noise limits of laser light. However, they are still limited by the quantum uncertainty of bright carrier beams. The GQuEST project[2] (Gravity from the Quantum Entanglement of Space Time) proposes a new approach called photon-counting interferometry. Instead of relying on

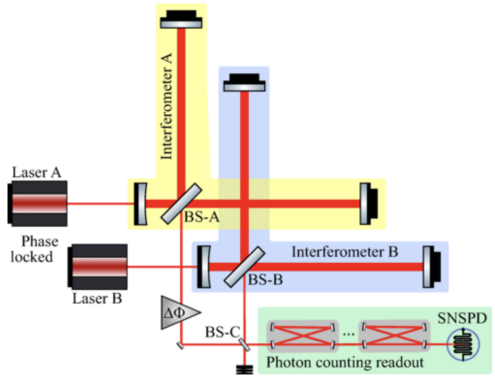

Figure 1: Simplified Design of the GQuEST Experiment

high laser power, GQuEST uses tuned cavities and photon-counting detectors to look for rare photons that carry possible signatures of spacetime fluctuations, while rejecting unwanted background light. To further improve sensitivity, the setup uses two interferometers in parallel (Figure 1). Any real geontropic signal should appear in both simultaneously, whereas local noise will not. This approach allows sensitivity to stochastic signals beyond the reach of classical interferometer designs.

The Rubidium Quantum Sensing (RbQ) project builds on GQuEST by incorporating laser-cooled ^{87}Rb atoms into the readout chain, transforming the interferometer into a hybrid quantum sensor. As the geontropic fluctuations imprint upon the laser as phase modulations, the light from the signal cavity will mainly be that from the carrier light from the laser with a very low amplitude side band[3] representing quantum gravity effects. Differentiating signal photons from the side band and the carrier photons is not feasible with photon counting alone, which is why GQuEST employs a series of optical filter cavities combined with a superconducting nanowire single-photon detectors (SNSPDs). In our approach, the ^{87}Rb atoms serve as a tunable filter cavity, enabling single photons to be converted into detectable atomic state changes. These atoms are first cooled and trapped in a 3D magneto-optical trap (3DMOT), then coupled to high-finesse optical cavities (Figure 2). The pump cavity, also referred to as the control, is tuned so that only photons with the signal that we expect from phase modulations in the interferometer will excite the atom into a specific hyperfine state, while all other photons are ignored. So when the signal photon enters the signal cavity, the excited atomic state is then detected with the projection drive. In this way, the atoms act as an extremely precise and tunable quantum filter, converting rare interferometer photons into detectable atomic state changes. In addition, atomic ensembles like this can provide access to non-Gaussian measurements. In addition, atomic ensembles like this can provide access to non-Gaussian measurements. While Gaussian squeezed states already surpass the standard quantum limit and are used at LIGO, non-Gaussian states can offer further advances for detecting weak, stochastic signals such as geontropic fluctuations.

The goal of this project is to determine how to design and tune the atom-cavity system so that signal photons from geontropic fluctuations can be detected with the highest possible accuracy. To support this, I built simulations that model rubidium as a Λ-type three-level atom and take a given signal pulse, representing the phase modulation from the interferome-

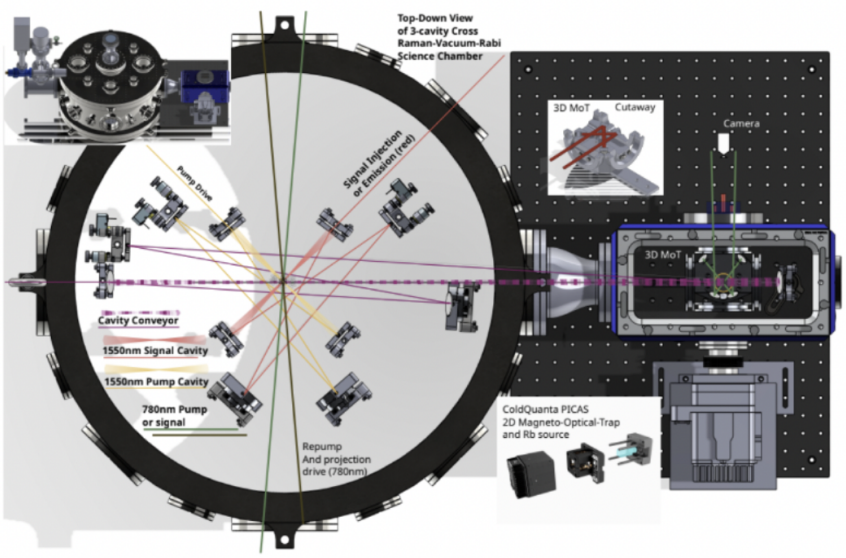

Figure 2: 3DMot and Chamber System with Multiple Crossed Cavities

ter, and calculate what kind of control pulse is needed to maximize detection. This involves exploring how cavity parameters such as loss, decay, and coupling interact with control pulse timing, frequency, and amplitude to enhance or suppress sensitivity. These results are intended to guide the design of RbQ by showing how carefully optimized control pulses and cavity settings can turn weak, gravitational induced signals into reliable, measurable events, making quantum-enhanced interferometer a practical tool for probing quantum gravity.

3 Theory

3.1 Atomic transitions

To understand how the atoms serve as a filter for detecting signal photons, it is useful to describe the relevant atomic transitions in more detail. The specific frequencies required to transition the atom from each state can be found in the Appendix 4[4]. The atom are first trapped and cooled in the $5^2S_{1/2}, F = 2, m_F = -2$ hyperfine state. The 3D MOT then drives the cycling transition $5^2S_{1/2}, F = 2, m_F = -2 \rightarrow 5^2P_{3/2}, F' = 3, m_F = -3$ (Figure 3). After excitation, the atom decays back down to the initial state, although selection rules occasionally allow decay into $F = 1$, a repump laser quickly returns the atom to $F = 2$ so the cycle continues.

Once the atoms are cooled and in the center of the cavity, the MOT beams are shut off and the atoms are optically pumped via the initialization laser into the $5^2S_{1/2}, F = 1, m_F = -1$ state labeled $|g_1\rangle$. The goal is to detect photons by transferring population from this state to $5^2S_{1/2}, F = 2, m_F = 1$ labeled $|g_2\rangle$. Direct population transfer between $|g_1\rangle$ and $|g_2\rangle$ is forbidden, since they belong to different hyperfine manifolds with no dipole-allowed single-

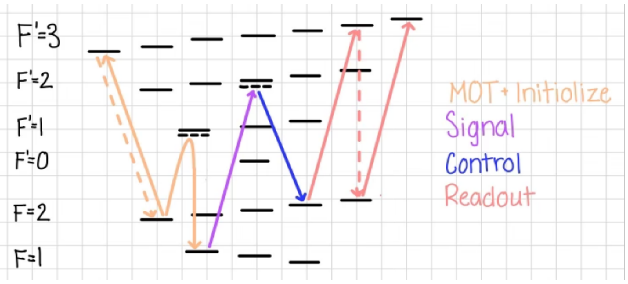

Figure 3: Atomic Transitions of ^{87}Rubidium Atom in Cavity

photon transition. Instead, we create an effective two-level system using a control laser and the incoming signal photon. Together, they drive a Raman process through an intermediate excited state $5^2P_{3/2}, F' = 2, m_F = 0$ labeled $|e\rangle$ allowing the atom to make the otherwise forbidden transition.

The effective two-level system is key to filtering. The Raman resonance condition requires that the control laser be tuned precisely relative to the signal photon frequency. In practice, this means that we calculate the expected frequency of the signal photon set by the interferometer's phase modulation and adjust the control laser so that the Raman transition $|g_1\rangle \rightarrow |g_2\rangle$ only occurs when that signal photon is present. This ensures that background light or photons at the wrong frequency do not trigger the transition which is key as the frequency from the laser will be much more powerful than that of the signal we are trying to detect.

Finally, the readout process brings the atom from $|g_2\rangle$ to $5^2P_{3/2}, F' = 3, m_F = 2$. When the atom decays down to $5^2P_{3/2}, F' = 3, m_F = 2$, it enters a cycling transition that emits many photons, providing an amplification mechanism. These photons can then be detected with high efficiency so a single signal photon leads to a strong, repeated fluorescence signature. In this way, the atom-cavity system functions as a frequency-selective quantum filter: a detection event occurs only when the incoming photon matches the tuned signal frequency.

3.2 Model Hamiltonians

The dynamics of the atom-cavity system are described by a Hamiltonian that includes both the coherent interactions with the cavity field and the effects of external driving fields. Different Hamiltonians were explored in simulation depending on the level of complexity required. To start, I used the Jaynes-Cummings Hamiltonian which models a single two-level atom interacting with a single cavity mode. This served as a baseline to test and validate my simulations:

$$H_{\text{JC}} = \omega_c a^\dagger a + \omega_s |e\rangle\langle e| + \Omega(a|e\rangle\langle g| + a^\dagger |g\rangle\langle e|) \tag{1}$$

where ω_c is the cavity frequency, a is the cavity annihilation operator, ω_s is the excited state frequency, Ω is the coupling strength between atom and cavity, and $|e\rangle$, $|g\rangle$ are the excited and ground states of the atom.

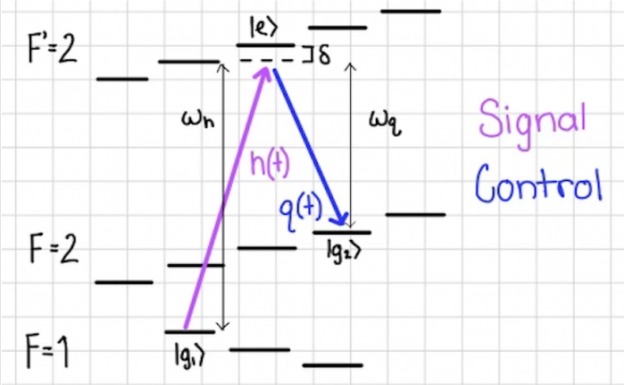

Figure 4: Λ-Type Three-Level System Representing the Signal-Control Transition

The time evolution of the system is governed by the Lindblad master equation:

$$\frac{d\rho}{dt} = -\frac{i}{\hbar}[H,\rho] + \sum_k \left(L_k \rho L_k^\dagger - \tfrac{1}{2}\{L_k^\dagger L_k, \rho\} \right), \tag{2}$$

where ρ is the density matrix of the system, H is the Hamiltonian, and L_K are the Lindblad (jump) operators that represent dissipative processes. In this case, the dominant processes are spontaneous emission from the atom and photon leakage from the cavity.

Moving beyond the two-level approximation, the full signal-control interaction in ^{87}Rb requires treating the atom as a three-level Λ-system with the ground states $|g_1\rangle$ and $|g_2\rangle$ coupled to an excited state $|e\rangle$ (Figure 4). The Hamiltonian in this is more complicated because it includes multiple coupling terms from both the signal and control fields. Solving the corresponding Lindblad equation directly can become unwieldy. To simplify the dynamics, we transform it into a rotating frame[5] aligned with the driving fields and cavity mode. Conceptually, this means moving into a reference frame that rotates at the frequency of the drive so that terms at that frequency are zeroed out (Appendix 5, 6, 7). The result is an effective Hamiltonian where only the physically relevant detunings and coupling strengths remain:

$$\tilde{H} = \Omega_1(e^{i\delta t} a\sigma_1^\dagger + e^{-i\delta t} a^\dagger \sigma_1) + (h(t)a^\dagger + h(t)^\dagger a) + (q(t)\sigma_2^\dagger + q(t)^\dagger \sigma_2) \tag{3}$$

where Ω_1 is the coupling strength between $|g_1\rangle$ and $|e\rangle$, δ is the detuning, and σ_1 and σ_2 are the annihilation operators of $|g_1\rangle$ and $|g_2\rangle$. The signal and control photon functions are $h(t)$ and $q(t)$ of the form

This effective Hamiltonian directly encodes how the control and signal pulses interact to drive population transfer between $|g_1\rangle$ and $|g_2\rangle$. By solving for the final atomic state, we can compute the probability that the atom ends in $|g_2\rangle$. The goal of the simulation is to find the control pulse shapes and cavity parameters that maximize this transfer probability, thereby making the atom-cavity system function as a precise and selective filter for geontropic signal photons.

3.3 Quantum Fisher Information

To evaluate how different parameters, such as cavity loss, decay rate, and the timing and frequency of the control signal, affect the atom's final state, I used the Quantum Fisher Information (QFI). QFI quantifies how sensitive a quantum state is to small changes in a parameter. A high QFI means that even a small change in the parameter produces a large, distinguishable change in the atomic states. For a quantum state $\rho(\theta)$ that depends on some parameter θ, the QFI is defined as

$$F_Q(\theta) = \mathrm{Tr}\left[\rho(\theta) L_\theta^2\right], \tag{4}$$

where L_θ is the symmetric logarithmic derivative (SLD) operator, defined through

$$\frac{\partial \rho(\theta)}{\partial \theta} = \frac{1}{2}\left(L_\theta \rho(\theta) + \rho(\theta) L_\theta\right). \tag{5}$$

By calculating F_Q for different cavity parameters and control pulse shapes, we can identifiy which parameters have the strongest influence on signal detection. This makes it possible to prioritize experimental precision where it matters most, ensuring that limited resources are directed towards controlling the parameters that most affect the ability to detect weak signals.

4 Methods

All simulations were carried out in Julia using the QuantumToolbox.jl package which provides tools for simulating open quantum systems. This framework is particularly useful because it allows direct construction of Hilbert spaces, operators, and time evolution with built-in solvers for the Lindblad master equation.

The system was built by first defining the Hilbert space of the atom-cavity system. For each model, I constructed the relevant atomic states (ground, excited), the cavity mode, and the associated operators such as annihilation/creation operators and projection operators onto atomic states. Time evolution was then computed with the "mesolve" function, which numerically integrates the Lindblad master equation for a given Hamiltonian and set of collapse operators. This made it possible to directly calculate the density matrix $\rho(t)$ at each time step, from which populations and expectation values were extracted.

To begin, I simulated a two-level atom coupled to a single cavity mode described by the Jaynes-Cummings Hamiltonian (Equation 1). Here, two coupling functions govern the interaction between the ground state and cavity and excited state and cavity. This simpler model provided a baseline to check that the simulation code behaved as expected. Because the two-level case has well-known analytic results for Rabi oscillations and cavity-atom exchange dynamics, it was a convenient way to verify that the solvers and operator definitions were working correctly. I preformed additional validation steps by deliberately choosing

parameters where the behavior was predictable - for example, removing coupling terms or drives and confirming the atom remained in its initial state.

After confirming the validity of the two-level simulations, I extended the model to a three-level Λ-type system, which is required to capture the signal-control interactions in ^{87}Rb. The Hamiltonian for this system (Equation 3) includes coupling terms from both the signal and control fields to the excited state, as well as dissipative processes from spontaneous emission and cavity losses. To check that the three-level model was implemented correctly, I tested for the presence of a dark state, a coherent superposition of the two ground states that does not couple to the excited state under the right signal-control conditions. In this state, destructive interference prevents excitation, leaving the atom "invisible" to the drive fields, an expected signature of Electromagnetically Induced Transparency (EIT). Detecting this dark state confirmed that the model reproduced the expected Λ-system physics (Appendix 3). Just as with the two-level system, I carried out further checks by setting parameters to known limits and verifying the outcome matched expectations. These tests consistently gave correct results, providing confidence that the three-level dynamics were simulated accurately.

With this framework in place, I was then able to simulate how different control pulse shapes and cavity parameters influenced the systems ability to register weak signal photons, directly supporting the project's goal of optimizing quantum-enhanced signal detection.

5 Results

5.1 Two-Level Atom System

I started by simulating a simplified two-level atom coupled to a cavity, with states $|g\rangle$ and $|e\rangle$. The atom-cavity coupling was driven by two time-dependent functions, $g_1(t)$ and $g_2(t)$, which governed the transfer of population from the ground state to the cavity and then from the cavity to the excited state. Both $g_1(t)$ and $g_2(t)$ were modeled as Gaussian pulses of the form

$$g(t) = b \exp\left(-\frac{(t-c)^2}{2d^2}\right) \tag{6}$$

thus b corresponds to amplitude, c to center of the pulse in time (ms), and d the width of the pulse (ms). Guassians were chosen because they resemble the shapes of the signal and control photons used in the full three-level system. The simulation started with the atom in $|g\rangle$, and by sequentially applying $g_1(t)$ and $g_2(t)$, I was able to confirm that the excitation process worked as expected. To ensure, numerical accuracy, I tested different Hilbert space sizes and found that a dimension greater than three was sufficient, since results stabilized beyond that point.

I then built a system where the user could set the parameters of the first pulse, $g_1(t)$, and obtain the optimal parameters of the second pulse, $g_2(t)$, by scanning over its height, width, and timing. For example, choosing $g_1(t)$ with parameters $b = 10, c = 0, d = 0.1242$

gives an optimal $g_2(t)$ at $b = 10.42, c = 0.3707, d = 0.0601$. This combination transfers population into $|e\rangle$ with a final value of 0.9897, which is high enough to be considered an efficient excitation (Appendix 1). More broadly, varying the pulse parameters and plotting the final $|e\rangle$ population showed that small changes in $g_1(t)$ or $g_2(t)$ can dramatically affect the outcome. This sensitivity is promising for using the atom - cavity system as a filter, since it means the atom will only transition when the signal photon matches the control tuning. I also tested whether the pulses should overlap in time, and found that overlap consistently produced higher transfer efficiency (Appendix 2). Together, these checks confirmed that the two-level simulations were behaving as expected and provided a solid baseline for extending the model to the more complex three-level system.

5.2 Three-Level Λ-Type Atom System

For the three-level Λ-type system, I constructed the rotated Hamiltonian described in Equation 3. In this case, the signal and control pulse function are of the form

$$h(t) = g_1(t) \times \sin(\omega_h t) \text{ and } q(t) = g_2(t) \times \sin(\omega_q t) \tag{7}$$

where ω_h and ω_q are the frequencies of the signal and control pulses respectively. To ensure accuracy, I tested different Hilbert space sizes and found that a dimension larger than 14 was required to avoid numerical artifacts.

Once the system was stable, I built a framework where the user could input the parameters of the signal pulse and obtain the optimal control pulse through a parameter scan. Here, the final state of $|g2\rangle$ is calculated to try and find parameters with the maximum $|g1\rangle \rightarrow |g2\rangle$ population transfer. For example, a signal pulse with $b = 5, c = 1, d = 0.15$, and $\omega_h = 1.555$ has an optimal control pulse with $b = 5.556, c = 1.264, d = 0.25$, and $\omega_h = 0.614$ (Appendix 10). To visualize the dynamics, I used Bloch-sphere plots of the atomic states and Wigner functions of the cavity field. These showed the expected population transfer into the cavity mode, and the Wigner function displayed the non classical features that confirmed the cavity photon field was being properly modeled. Another important check was time-reversal symmetry: starting the system in the second ground state and applying the optimized control pulse in reverse reproduced the original signal photon. This confirmed that the control pulse was indeed optimal, since it inverted the process.

I also explored how the signal and control photon frequencies affected the outcome. The results showed that transitions only occurred for very specific signal–control frequency pairs (Figure 5). This is a very promising result as it indicates that when setting the control frequency, only signal photons with a specific frequency will allow the $|g1\rangle \rightarrow |g2\rangle$ transition. Thus the system will only accept the signal photon and reject all others acting as a frequency filter.

Finally, I computed the QFI for the three-level system. The results showed that varying the signal photon parameters consistently gave QFI values about twice as large as those from varying the control parameters, indicated that the system is most sensitive to signal input.

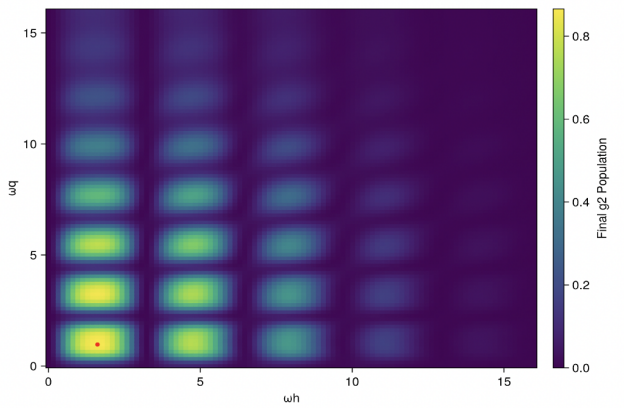

Figure 5: Varying Frequencies of Signal and Control Pulses vs End State Value

Cavity losses were also found to have over a hundred times higher QFI than atomic decay rates, suggesting imperfections in the cavity are the main limitation for detection efficiency. Together, these results show that the atom-cavity system can act as a tunable quantum filer - when the signal photon matches the optimized control photon, population transfer occurs reliably, but even small deviations prevent the transition allowing selective detection.

6 Conclusion

In this work, I developed simulations of atom–cavity systems to optimize the interaction between signal photons and control pulses, directly supporting the Rubidium Quantum Sensing (RbQ) project. I demonstrated that for both two-level and three-level Λ-type ^{87}Rb atom systems, it is possible to tailor the control pulse to a given signal pulse in order to maximize population transfer to the target atomic state. This provides a proof of concept that the atom–cavity system in RbQ can act as a highly selective quantum filter, detecting only those photons that match the optimized control pulse.

These simulations also established a foundation for more advanced cavity models. By incorporating additional features such as more realistic cavity parameters, multiple modes, or readout schemes, this framework can be extended to guide experimental designs for RbQ and other quantum-enhanced sensing platforms. Future work will focus on optimizing control pulses in the frequency domain rather than solely in the time domain, which is a crucial step for detecting geontropic fluctuations as they are predicted in frequency space.

Overall, these results demonstrate that simulation-driven tuning of the atom–cavity interactions can enhance the sensitivity and selectivity of RbQ. This approach provides a practical pathway for using quantum-enhanced measurements to detect faint signals from tabletop interferometers, bringing us closer to probing quantum gravitational effects in the laboratory.

7 References

1. Verlinde, Erik P, and Kathryn M Zurek. "Observational Signatures of Quantum Gravity in Interferometers." Physics Letters B, vol. 822, 1 Nov. 2021, pp. 136663–136663, https://doi.org/10.1016/j.physletb.2021.136663. Accessed 19 Mar. 2024.

2. Vermeulen, Sander M., et al. "Photon-Counting Interferometry to Detect Geontropic Space-Time Fluctuations with GQuEST." Physical Review X, vol. 15, no. 1, 14 Feb. 2025, https://doi.org/10.1103/physrevx.15.011034.

3. Black, Eric D. "An Introduction to Pound–Drever–Hall Laser Frequency Stabilization." *American Journal of Physics*, vol. 69, no. 1, Jan. 2001, pp. 79–87, https://doi.org/10.1119/1.1286663

4. Steck, Daniel. Rubidium 87 D Line Data. 2001.

5. Daniel Adam Steck. Quantum and Atom Optics. 2007.

6. Sen, Surajit, et al. "Comparison of Electromagnetically Induced Transparency in Lambda, Cascade and Vee Three-Level Systems." Journal of Modern Optics, vol. 62, no. 3, 30 Sept. 2014, pp. 166–174, https://doi.org/10.1080/09500340.2014.960019. Accessed 30 May 2024.

7. Khademi, Siamak, et al. "An Exact Scheme for the EIT for a Three-Level Λ -Type Atom in a Quantum Cavity." Appl. Math. Inf. Sci, vol. 9, no. 3, 2015, pp. 1225–1229, www.naturalspublishing.com/files/published/9n353oj2ti8577.pdf, https://doi.org/10.12785/amis/090 Accessed 22 Sept. 2025.

8. Dilley, Jerome, et al. "Single-Photon Absorption in Coupled Atom-Cavity Systems." Physical Review A, vol. 85, no. 2, 24 Feb. 2012, https://doi.org/10.1103/physreva.85.023834. Accessed 18 Mar. 2021.

9. Gorshkov, Alexey V, et al. *Photon Storage in Λ-Type Optically Dense Atomic Media. II. Free-Space Model.* Vol. 76, no. 3, 7 Sept. 2007, https://doi.org/10.1103/physreva.76.033805. Accessed 16 May 2023.

10. Allen, Richard R, et al. "Quantum Computing Enhanced Sensing." ArXiv (Cornell University), 13 Jan. 2025, https://doi.org/10.48550/arxiv.2501.07625.

11. Avikar Periwal, et al. "Programmable Interactions and Emergent Geometry in an Array of Atom Clouds." Nature, vol. 600, no. 7890, 22 Dec. 2021, pp. 630–635, https://doi.org/10.1038/s41586-021-04156-0.

8 Acknowledgements

This work was supported by the National Science Foundation (NSF), the LIGO Laboratory Summer Undergraduate Research Fellowship program (LIGO SURF), and the California Institute of Technology Student-Faculty Programs.

9 Appendix

1. Maximizing Transfer of Energy of 1 Cavity 2 Atom System

[Reilly, Jeff]

Building 1 Cavity and 2 Atom System

Started off by changing the parameters, operators, initial state, and collapse operators to accommodate such a system. Instead of using a driving force on the cavity that changes with time, I had the coupling between the atoms and cavity change with time. The coupling was represented by time dependent functions that were made into quantum objects and added to the hamiltonian.

Changing the Expectation Value Calculation

The last expectation value calculation worked by calculating the state from 0 to t for every t in tlist and saving the final t in a list. I changed it to only calculate the state once from 0 to the end time and save each iteration to a list. I did the same thing again but with the parameter shifted by a fraction and the iterated through each list to find teh derivative. aThen I used both to calculate the expectation values in a much more efficient way than before.

Maximizing the Transfer of Energy

After trying a variety of shapes for the functions describing the atom 1 to cavity (g1(t)) and cavity to atom 2 (g2(t)) coupling, I found using Gaussians worked the best. Then I wrote a function that goes through a range of values for each and plotted the spin of the 2nd atom vs. the value of the parameter. The plots are shown below were b, c, and d correspond to the Gaussian's height, position, and width respectively.

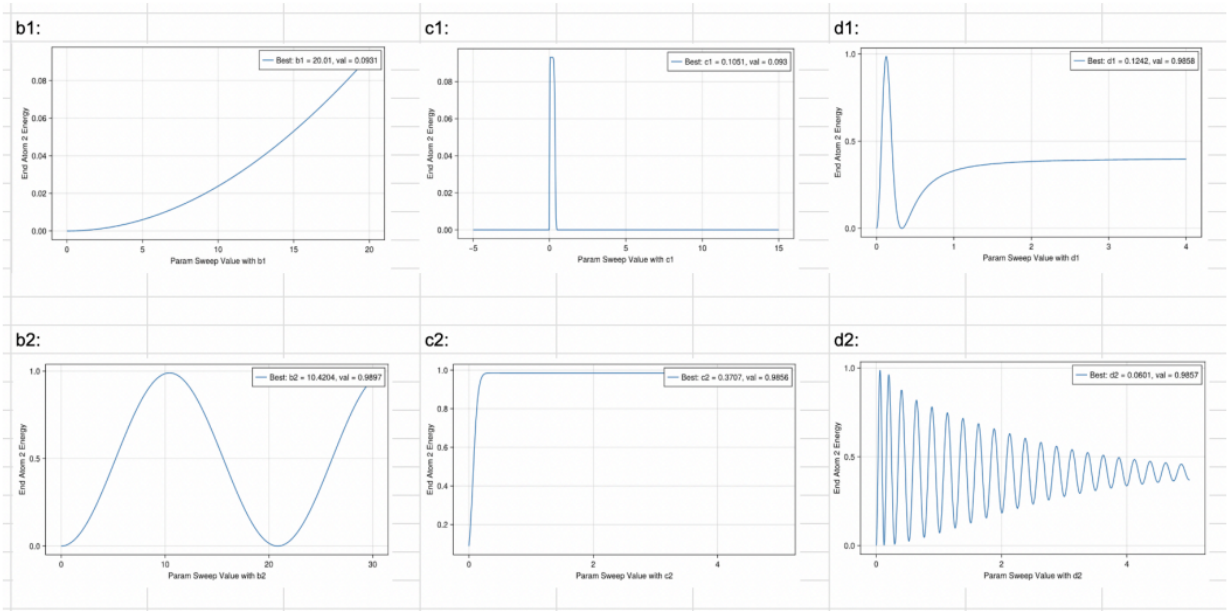

I found the optimal parameters to be as shown below along with the expectation values and g functions per time.

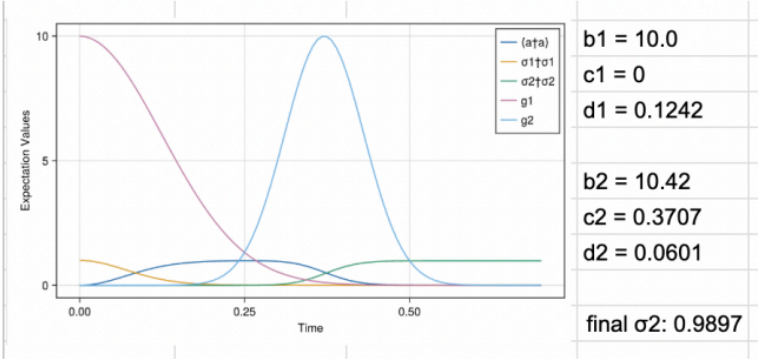

The final spin of the second atom here is 0.9897. The goal would be to have a = 0, σ1 = 0, and σ2 = 1 but instead we have a = 0.0038, σ1 = 0.0061, and σ2 = 0.9897 which isn't perfect but as close as I could get.

Varying multiple parameters against each other and finding the final |e> value renders the following plot:

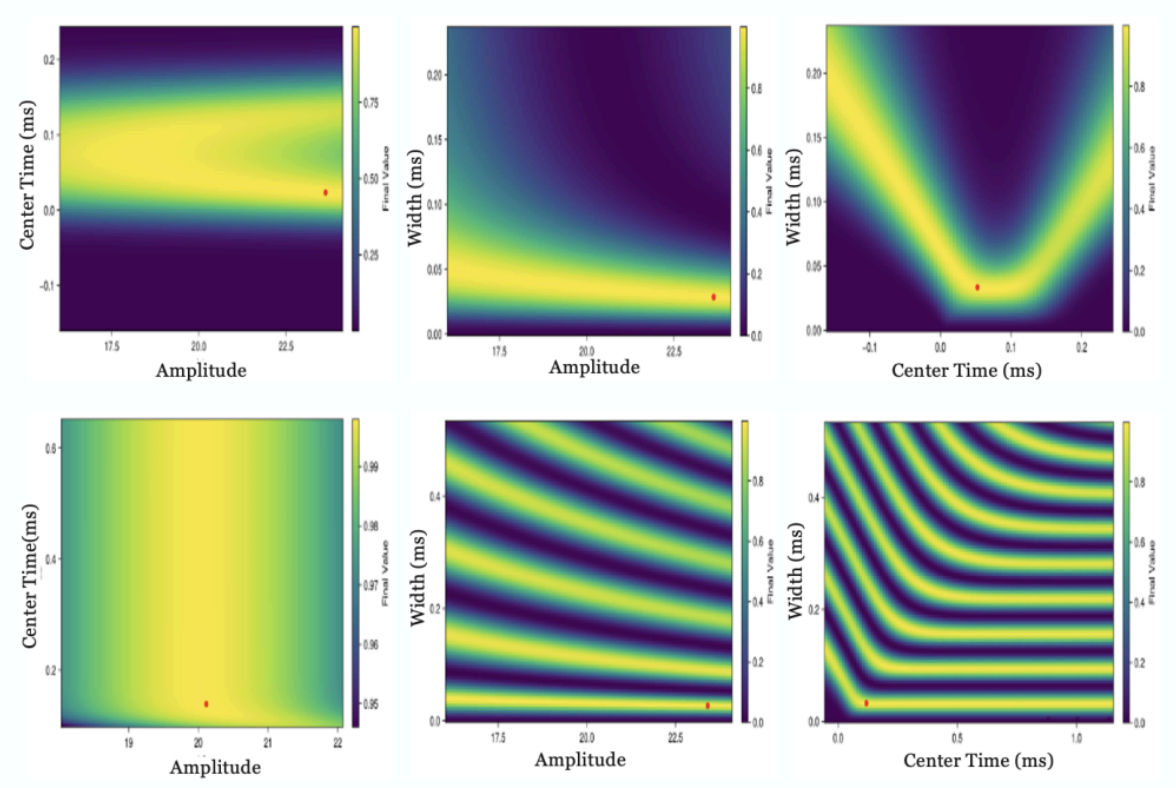

Interesting to see how small changes in width of second pulse can dramatically change the final |e> value.

2. Overlapped vs. Nonoverlapped Coupling Curves

[Reilly, Jeff]

Comparison of end-state results for a two-level, two-atom, one-cavity system under varying coupling profiles, keeping amplitudes below 20. For each configuration, parameters were optimized to maximize the final excitation probability of the second atom. The configuration with partially overlapping coupling curves had the highest final excitation, though only by a margin of 0.00015.

Non-Overlapped

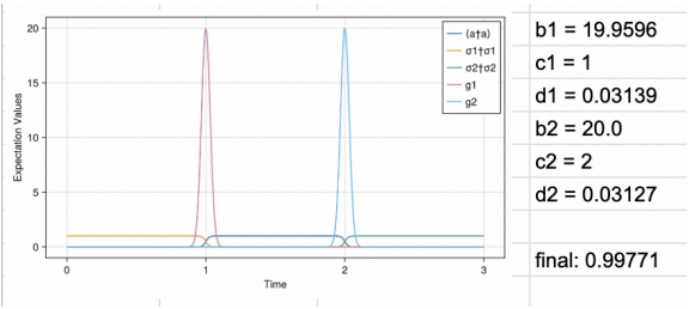

Entirely Overlapped

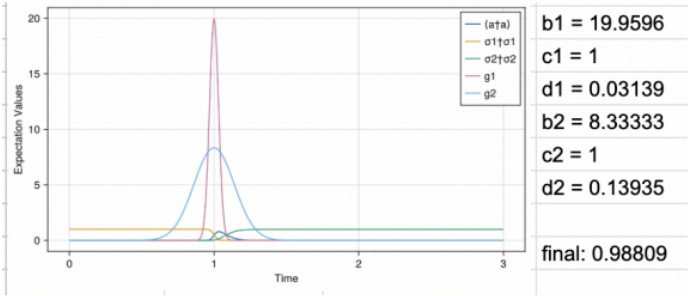

Partially Overlapped

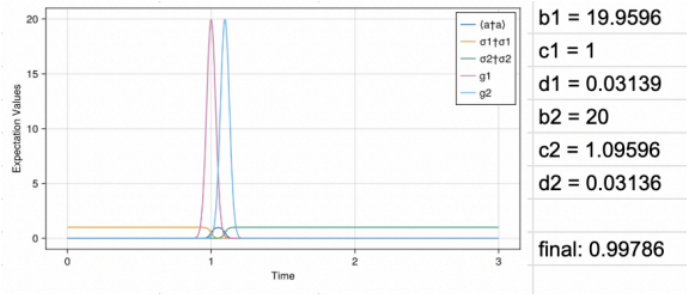

Interesting Results from Overlap vs. Width of Guassian

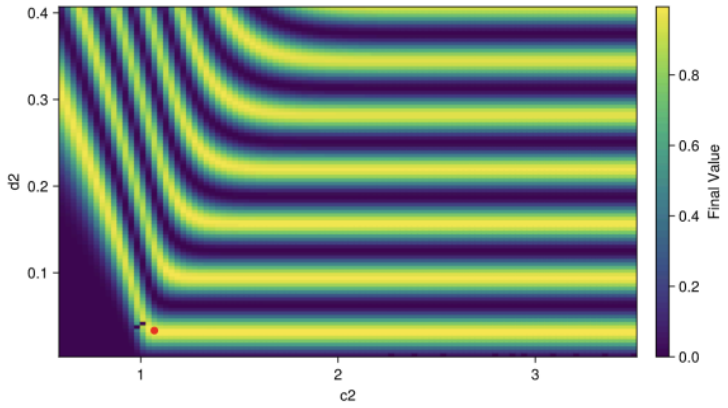

3. Frequency Sweep to Find Dark State

[Reilly, Jeff]

Simulated three level ƛ type atom in cavity with the following structure:

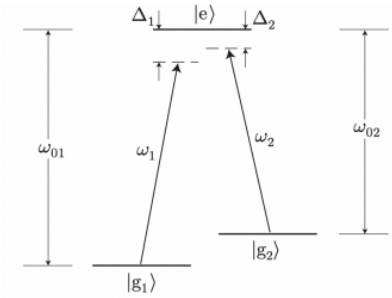

Using the following hamiltonians (in rotated frame of the frequency of e state thats why squiggly)

$$H_A = \hbar\Delta_1|g_1\rangle\langle g_1| + \hbar\Delta_2|g_2\rangle\langle g_2|$$
$$\tilde{H}_{AF} = \frac{\hbar}{2}\Omega_1(\sigma_1 + \sigma_1^\dagger) + \frac{\hbar}{2}\Omega_2(\sigma_2 + \sigma_2^\dagger)$$

where HA = hamiltonian of free atom and HAF = hamiltonian of atom-field interactions. Note:

1. $\Omega_\alpha := \frac{-\langle g_\alpha|\hat{\varepsilon}_\alpha \cdot \mathbf{d}|e\rangle E_{0\alpha}}{\hbar}$ but I am using set values cause I think can find in documentation the actual value
2. $\sigma_1 = |g_n\rangle\langle e|$ is what I found in text but may want to change this - will look at Quantum Mechanics textbook

Also used `pss = steadystate(H, collapse)` instead of mesolve because this found the steady state instead of solving for a really long time until the states settled. Also used `collapse = [√Γ1 * σ1, √Γ2 * σ2]` for collapse operators - when putting into steadystate I think it applies D[σn]. Steck said I should get something like:

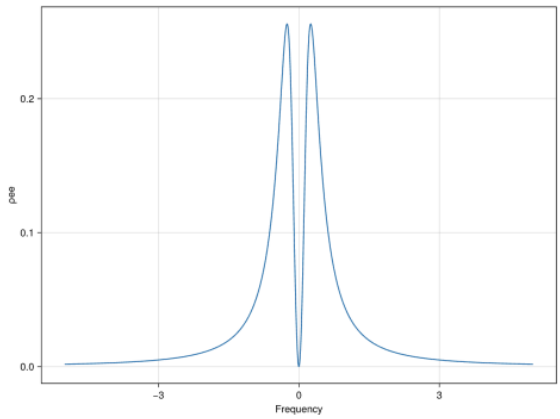

which is pretty good so hooray!

4. Calculating Rb Atom Frequencies

[Reilly, Jeff]

I used Steck's Rb doc (link) to find the frequencies required to excite the atom from `|g1⟩` to `|e⟩` (from the signal photon - h(t)) and `|e⟩` to `|g2⟩` (from the control - q(t)). The black arrows showing the splitting between hyperfine (F) levels are from steck. This is the frequency required to go between states with no magnetic field. When a magnetic field is present, the magnetic sub levels (mF) start to diagnalize causing the splitting of states shown in the picture. The way to calculate the new frequency required to go between states is by using Zeeman splitting (link). The change in energy of the sub levels is calculated by

$$\Delta E = m_F g_F B.$$

Thus the following calculation is used to find the required frequency for h(t):

$$\begin{aligned}\omega_{h(t)} &= \omega_h + \Delta E \\ &= \omega_h + [(m_{F'=2} g_{F'=2} B) - (m_{F=1} g_{F=1} B)] \\ &= \omega_h + [(0)(0.93\,\mathrm{MHz/G})B - (-1)(-0.07\,\mathrm{MHz/G})B]^{\cdot} \\ &= \omega_h - 0.07\,\mathrm{MHz/G} \cdot B\end{aligned}$$

A similar calculation is done for q(t).

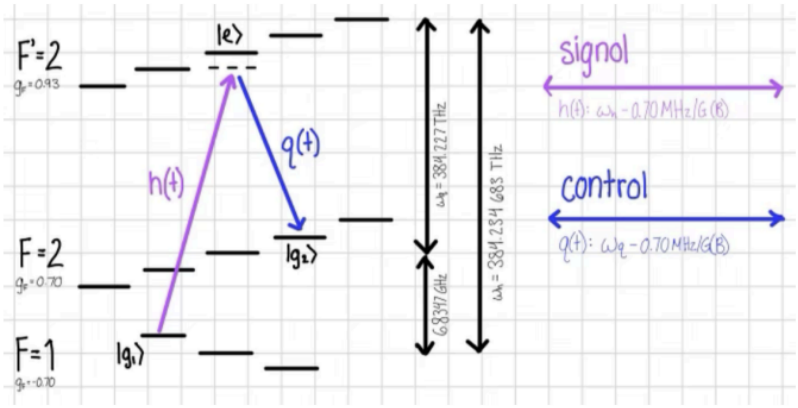

Thus the required frequency for h(t) and q(t) are ωh - 0.07MHz/G*B and ωq - 0.07MHz/G*B respectively. The greater the magnitude of B, the greater the separation between magnetic sub levels. By changing B and thus the frequency of h(t), you change what frequency will be absorbed by the atom and thus what frequency RbQ is detecting for. As the sidebands of the total signal returning to the cavity will be wide, this ability to tune what frequency we are search for mid experiment will be helpful to gather more data about the shape of the gravitational signal.

5. Non-Rotating Hamiltonian of Signal-Control Interaction

[Reilly, Jeff]

I made a Hamiltonian describing the Rb atom during the stage where it is excited by the signal photon and then brought down by the control field. As shown in the diagram, the atom is first controlled by the 3D-MOT and then initialized using STIRAP. Next it is excited by the signal photon and brought back down by the control field. Finally it goes through a series of transitions during the readout phase where the decay from F′=3 to F=2 emits a photon that we detect.

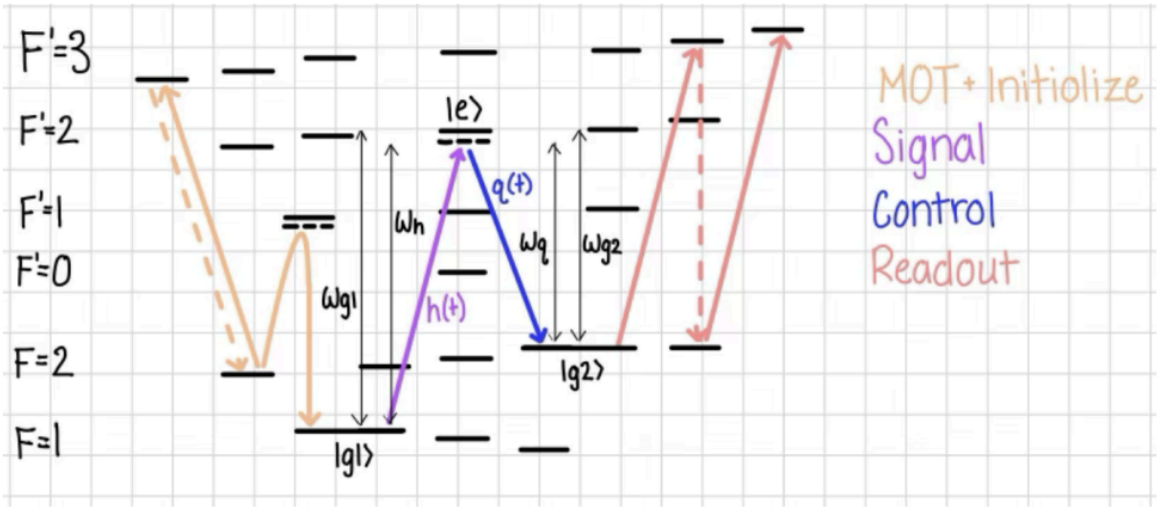

The Hamiltonian describes the transition from the g1 state to e driven by the signal photon and e to g2 driven by the control. It looks like

$$H = H_{\text{atom}} + H_{\text{cav}} + H_{\text{int}} + H_{\text{sig}}(t) + H_{\text{control}}(t).$$

Hatom describes the atom in free space:

$$H_{\text{atom}} = \hbar\omega_{g1}|g1\rangle\langle g1| + \hbar\omega_{g2}|g2\rangle\langle g2| + \hbar\omega_{e}|e\rangle\langle e|.$$

Hcav describes just the cavity:

$$H_{\text{cav}} = \hbar\omega_{\text{cav}}(a^{\dagger}a) = \hbar\omega_{h}(a^{\dagger}a).$$

ωcav is approximately ωh here because we want the signal to be in resonance with the cavity. Hint describes the interaction between the atom and the cavity and is:

$$H_{\text{int}} = \hbar\Omega_1(\sigma_1 a^{\dagger} + \sigma_1^{\dagger}a) + \hbar\Omega_2(\sigma_2 a^{\dagger} + \sigma_2^{\dagger}a)$$

where Ωn describes the coupling strength between gn and e and, a is the annihilation operator for the cavity, and σn is the lowering operator |e> → |gn> and thus σn = |gn><e|. The σ*adagger represents energy going from the atom to the cavity as the lower operator is placed on the atom

and the dagger of the annihilation operator is placed on the cavity. The σdagger*a represents the reverse process. Hsig(t) describes the Hamiltonian of the signal photon:

$$H_{\text{sig}}(t) = \hbar(a + a^{\dagger})h(t) \text{ where } h(t) = A_1 \sin(\omega_h t).$$

Here A1 is a gaussian and h(t) represents the signal photon. The photon only interacts with the cavity and then the atom will absorb it through the interaction Hint. Finally, Hcontrol(t) describes the control field within the cavity:

$$H_{\text{control}} = \hbar(e^{i\omega_q t}\sigma_2 + e^{-i\omega_q t}\sigma_2^{\dagger})q(t) \text{ where } q(t) = A_2 \sin(\omega_q t).$$

A2 is a gaussian and q(t) represents the control field. This field is only resonant with the e → g2 transition which is why only σ2 is involved.

6. Rotating Jaynes-Cummings Hamiltonian

[Reilly, Jeff]

We set out to rotate the Jaynes-Cummings Hamiltonian to understand how to rotate the Hamiltonian used for the Rb-cavity system to simplify terms in the simulation. To begin with, the Jaynes-Cummings Hamiltonian (note hbar = 1):

$$H_{\mathrm{JC}} = \omega_c a^\dagger a + \omega_s |e\rangle\langle e| + \Omega(a|e\rangle\langle g| + a^\dagger |g\rangle\langle e|)$$

where ωc is the cavity frequency, a is the cavity annihilation operator, ωs is the excited state frequency, Ω is the coupling strength between atom and cavity, and |e> and |g> are the excited and ground states respectively. We end up with a final rotated Hamiltonian

$$\tilde{H} = \Omega(e^{i(\omega_s-\omega_c)t} a|e\rangle\langle g| + e^{-i(\omega_s-\omega_c)t} a^\dagger |g\rangle\langle e|).$$

Here is how we did it:

1. **ROTATE WITH ATOM**

The first step is to rotate the atom. Thus is done using the following formula from steck (link)

$$\tilde{\mathrm{H}} = \mathrm{UHU}^\dagger + i\hbar(\frac{d}{dt}\mathrm{U})\mathrm{U}^\dagger$$

where Htilde is the rotated Hamiltonian. To rotate that Hamiltonian with the atom,

$$\mathrm{U} = e^{i\omega_s t|e\rangle\langle e|}$$

so that it is rotating at the atom spin ωs and effects things in |e>. First, note that

$$\frac{d}{dt}\mathrm{U} = i\omega_s|e\rangle\langle e|e^{i\omega_s t|e\rangle\langle e|} = i\omega_s|e\rangle\langle e|\mathrm{U}$$

$$\text{and}$$

$$\mathrm{U}^\dagger = e^{-i\omega_s t|e\rangle\langle e|}.$$

Thus,

$$i\hbar(\frac{d}{dt}\mathrm{U})\mathrm{U}^\dagger = i(i\omega_s|e\rangle\langle e|e^{i\omega_s t|e\rangle\langle e|})e^{-i\omega_s t|e\rangle\langle e|} = i(i\omega_s|e\rangle\langle e| = -\omega_s|e\rangle\langle e|.$$

Next, we look at the UHU† term. Note that by expanding out the taylor series,

$$\mathrm{U}|e\rangle = e^{i\omega_s t|e\rangle\langle e|}|e\rangle = (1 + i\omega_s t|e\rangle\langle e| + ...)|e\rangle = |e\rangle + i\omega_s t|e\rangle + ... = e^{i\omega_s t}|e\rangle,$$
$$\langle e|\mathrm{U}^\dagger = \langle e|e^{-i\omega_s t|e\rangle\langle e|} = \langle e|(1 - i\omega_s t|e\rangle\langle e| + ...) = \langle e| + i\omega_s t\langle e| + ... = e^{-i\omega_s t}\langle e|,$$
$$\mathrm{U}|g\rangle = e^{i\omega_s t|e\rangle\langle e|}|g\rangle = (1 + i\omega_s t|e\rangle\langle e| + ...)|g\rangle = |g\rangle + i\omega_s t|e\rangle\langle e|g\rangle + ... = |g\rangle,$$

$$\text{and}$$

$$\langle g|\mathrm{U} = \langle g|e^{-i\omega_s t|e\rangle\langle e|} = \langle g|(1 + i\omega_s t|e\rangle\langle e| + ...) = \langle g| - i\omega_s t\langle g|e\rangle\langle e| + ... = \langle g|$$

because, as this atom is described with an orthonormal basis, <g|e> = 0 and <e|e> = 1. Note that [|e><e|, a] = 0 as the two operators are manipulating two different things (the excited state of the

atom and cavity) and thus

$$\begin{aligned} UaU^\dagger &= (1 + i\omega_s t|e\rangle\langle e| + ...)a(1 - i\omega_s t|e\rangle\langle e| + ...) \\ &= (a + i\omega_s t|e\rangle\langle e|a + ...)1 - i\omega_s t|e\rangle\langle e| + ...) \\ &= a + i\omega_s t|e\rangle\langle e|a - i\omega_s ta|e\rangle\langle e| + ...) \\ &= a + i\omega_s t[|e\rangle\langle e|, a] + ... = a. \end{aligned}$$

A similar calculation can be done to show $Ua^\dagger U^\dagger = a^\dagger$ and thus $Ua^\dagger aU^\dagger = a^\dagger a$. Rotating the Hamiltonian with the atom will have no effect on the cavity operators. And so finally, looking at the total Hamiltonian, we have that

$$\begin{aligned} \tilde{\mathrm{H}}_{JC} &= \mathrm{UHU}^\dagger + i\hbar(\frac{d}{dt}\mathrm{U})\mathrm{U}^\dagger \\ &= \mathrm{U}(\omega_c a^\dagger a + \omega_s|e\rangle\langle e| \ + \ \Omega(a|e\rangle\langle g| + a^\dagger|g\rangle\langle e|)\mathrm{U}^\dagger \ - \ \omega_s|e\rangle\langle e| \\ &= \omega_c a^\dagger a \ + \ \omega_s e^{i\omega_s t}|e\rangle\langle e|e^{-i\omega_s t} \ + \ \Omega(ae^{i\omega_s t}|e\rangle\langle g| + a^\dagger|g\rangle e^{-i\omega_s t}\langle e|) \ - \ \omega_s|e\rangle\langle e| \\ &= \omega_c a^\dagger a \ + \ \Omega(e^{i\omega_s t}a|e\rangle\langle g| + e^{-i\omega_s t}a^\dagger|g\rangle\langle e|). \end{aligned}$$

Thus that is the Hamiltonian rotated with the atom.

2. ROTATE WITH CAVITY

The next step is to rotate the Hamiltonian with the cavity. Here,

$$\mathrm{U} = e^{i\omega_c t a^\dagger a}$$
$$\text{thus}$$
$$\mathrm{U}^\dagger = e^{-i\omega_c t a^\dagger a}$$
$$\text{and finally}$$
$$i\hbar(\frac{d}{dt}\mathrm{U})\mathrm{U}^\dagger = -\omega_c t a^\dagger a.$$

Now we look at $UaU^\dagger$. First, note that Hadamard's Lemma (link) states that

$$e^A B e^{-A} = B + [A, B] + \frac{1}{2!}[A, [A, B]] + \frac{1}{3!}[A, [A, [A, B]]] + ...$$

Thus in our $UaU^\dagger$ situation, we have that

$$A = i\omega_c t a^\dagger a \ \text{ and } \ B = a.$$

Using commutator identities (link),

$$[A, B] = [i\omega_c t a^\dagger a, a] = i\omega_c t[a^\dagger a, a] = i\omega_c t(a^\dagger[a, a] + [a^\dagger, a]a) = i\omega_c t(0 - a) = -i\omega_c ta$$
$$\text{and thus}$$
$$[A, [A, B]] = [i\omega_c t a^\dagger a, [i\omega_c t a^\dagger a, a]] = [i\omega_c t a^\dagger a, -i\omega_c ta] = (\omega_c t)^2[a^\dagger a, a] = -(\omega_c t)^2 a$$

Continuing with this process gives

$$\mathrm{UaU}^\dagger = e^{i\omega_c t a^\dagger a} a e^{i\omega_c t a^\dagger a} = a - i\omega_c ta - \frac{1}{2!}(\omega_c t)^2 a + \frac{1}{3!}i(\omega_c t)^3 a + ... = e^{-i\omega_c t}a.$$

Similar calculations can be done for $a^\dagger$ to show that $Ua^\dagger U^\dagger$ is the complex conjugate of $UaU^\dagger$. It can also be shown that $U|g\rangle\langle e|U^\dagger$ and $U|e\rangle\langle g|U^\dagger$ equal $|g\rangle\langle e|$ and $|e\rangle\langle g|$ respectively using a similar

method to that used in part 1 where we calculated UaU†. Rotating the Hamiltonian with the cavity will have no effect on the operators of the atom. Thus applying this rotation to our Hamiltonian gives

$$\begin{aligned}\tilde{\mathrm{H}}_{JC} &= \mathrm{UHU}^{\dagger} + i\hbar(\frac{d}{dt}\mathrm{U})\mathrm{U}^{\dagger} \\ &= U(\omega_c a^{\dagger}a \; + \; \Omega(e^{i\omega_s t}a|e\rangle\langle g| + e^{-i\omega_s t}a^{\dagger}|g\rangle\langle e|))U^{\dagger} - \omega_c t a^{\dagger}a \\ &= \omega_c(e^{-i\omega_c t}a^{\dagger})(e^{i\omega_c t}a) \; + \; \Omega(e^{i\omega_s t}(e^{-i\omega_c t}a)|e\rangle\langle g| + e^{-i\omega_s t}(e^{i\omega_c t}a^{\dagger})|g\rangle\langle e|) - \omega_c t a^{\dagger}a \\ &= \Omega(e^{i(\omega_s-\omega_c)t}a|e\rangle\langle g| + e^{-i(\omega_s-\omega_c)t}a^{\dagger}|g\rangle\langle e|).\end{aligned}$$

Thus that is our final Hamiltonian! Hooray! The closer ωs and ωc are in value, the more we can ignore the e terms and if they are equal e disappears all together which would be very nice.

7. Rotating Signal-Control Hamiltonian

[Reilly, Jeff]

Last rotated Hamiltonian for the signal-control process seemed fishy when simulating so we revisited. Fishiest part seemed to be the frequencies as setting ωe = 0 caused some logic issues where ωh = ωq which is impossible given g1 and g2 are on different hyperfine state levels and the detuning from e is the same for both drives. Thus we set out to rebuild the Hamiltonian by setting ωg1 = 0 from the beginning. The system is shown in the diagram below.

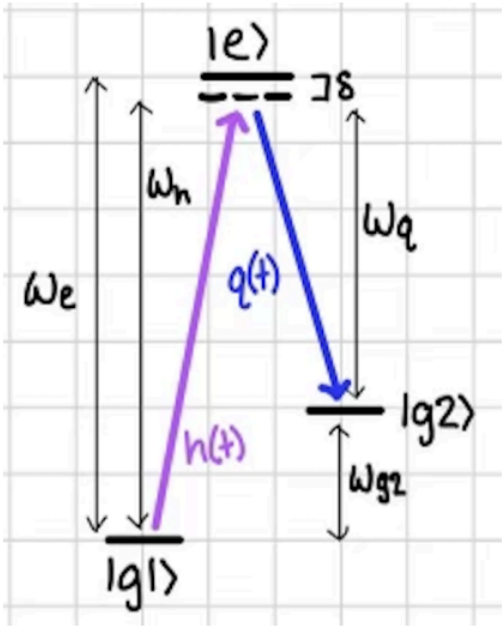

The resulting Hamiltonian for the system rotated with the cavity, state e, and state g2 is

$$\tilde{H} = \Omega_1(e^{i\delta t}a\sigma_1^\dagger + e^{-i\delta t}a^\dagger\sigma_1) + (h(t)a^\dagger + h(t)^\dagger a) + (q(t)\sigma_2^\dagger + q(t)^\dagger\sigma_2)$$

where Ω1 is the coupling strength between e and g1, a is the cavity annihilation operator, h(t) and q(t) are the signal photon and control functions respectively, and σn is the lowering operator e→gn (|gn><e|). Here is how it was calculated.

1. ROTATE WITH CAVITY

First, the Hamiltonian for this system is as follows:

$$H = \omega_{g2}|g2\rangle\langle g2| + \omega_e|e\rangle\langle e| + \omega_c a^\dagger a + \Omega_1(a|e\rangle\langle g1| + a^\dagger|g1\rangle\langle e|) + \Omega_2(a|e\rangle\langle g2| + a^\dagger|g2\rangle\langle e|)$$
$$+(h(t)a^\dagger + h(t)^\dagger a) + (q(t)|e\rangle\langle g2| + q(t)^\dagger|g2\rangle\langle e|).$$

The rotated Hamiltonian can be calculated using

$$\tilde{\mathrm{H}} = \mathrm{UHU}^\dagger + i(\frac{d}{dt}\mathrm{U})\mathrm{U}^\dagger \text{ where } U = e^{i\omega t|\psi\rangle\langle\psi|}.$$

To rotate with the cavity,

$$U = e^{i\omega_c t a^\dagger a}.$$

Looking at calculations done in Rotating Jaynes-Cummings Hamiltonian, we find that

$$U|g \text{ or } e\rangle U^\dagger = |g \text{ or } e\rangle,\ U\langle g \text{ or } e|U^\dagger = \langle g \text{ or } e|,\ UaU^\dagger = e^{-i\omega_c t}a,$$
$$Ua^\dagger U^\dagger = e^{i\omega_c t}a,\ \text{ and } i(\frac{d}{dt}\mathrm{U})\mathrm{U}^\dagger = -\omega_c a^\dagger a.$$

Note that because we want the signal photon to be resonant with the cavity, ωc = ωh. Thus the new rotate Hamiltonian becomes

$$H = \omega_{g2}|g2\rangle\langle g2| + \omega_e|e\rangle\langle e| + \Omega_1(e^{-i\omega_h t}a|e\rangle\langle g1| + e^{i\omega_h t}a^\dagger|g1\rangle\langle e|) + \Omega_2(e^{-i\omega_h t}a|e\rangle\langle g2|$$
$$+e^{i\omega_h t}a^\dagger|g2\rangle\langle e|) + (h(t)e^{-i\omega_h t}a^\dagger + h(t)^\dagger e^{-i\omega_h t}a) + (q(t)|e\rangle\langle g2| + q(t)^\dagger|g2\rangle\langle e|).$$

2. ROTATE WITH EXCITED STATE

Now

$$U = e^{i\omega_e t|e\rangle\langle e|}$$

and thus

$$U(|g\rangle, \langle g|, a, \text{ or } a')U' = (|g\rangle, \langle g|, a, \text{ or } a'),\ U|e\rangle U' = e^{i\omega_e t}|e\rangle,$$
$$U\langle e|U^\dagger = e^{-i\omega_e t}\langle e|,\ \text{ and } i(\frac{d}{dt}\mathrm{U})\mathrm{U}^\dagger = -\omega_e|e\rangle\langle e|.$$

The new Hamiltonian then becomes

$$H = \omega_{g2}|g2\rangle\langle g2| + \Omega_1(e^{-i(\omega_h-\omega_e)t}a|e\rangle\langle g1| + e^{i(\omega_h-\omega_e)t}a^\dagger|g1\rangle\langle e|)$$
$$+\Omega_2(e^{-i(\omega_h-\omega_e)t}a|e\rangle\langle g2| + e^{i(\omega_h-\omega_e)t}a^\dagger|g2\rangle\langle e|) + (e^{i\omega_h t}h(t)a^\dagger + e^{-i\omega_h t}h(t)^\dagger a)$$
$$+(e^{i\omega_e t}q(t)|e\rangle\langle g2| + e^{-i\omega_e t}q(t)^\dagger|g2\rangle\langle e|).$$

3. ROTATE WITH G2

Finally, to rotate with the g2 state,

$$U = e^{i\omega_{g2} t|g2\rangle\langle g2|}$$

and thus

$$U(|g1\rangle, \langle g1|, |e\rangle, \langle e|, a, \text{ or } a^\dagger)U^\dagger = (|g1\rangle, \langle g1|, |e\rangle, \langle e|, a, \text{ or } a^\dagger),\ U|g2\rangle U^\dagger = e^{i\omega_e t}|g2\rangle,$$
$$U\langle g2|U^\dagger = e^{-i\omega_e t}\langle g2|,\ \text{ and } i(\frac{d}{dt}\mathrm{U})\mathrm{U}^\dagger = -\omega_{g2}|g2\rangle\langle g2|.$$

The new Hamiltonian is then

$$H = \Omega_1(e^{-i(\omega_h-\omega_e)t}a|e\rangle\langle g1| + e^{i(\omega_h-\omega_e)t}a^\dagger|g1\rangle\langle e|) + \Omega_2(e^{-i(\omega_h-\omega_e+\omega_{g2})t}a|e\rangle\langle g2|$$
$$+e^{i(\omega_h-\omega_e+\omega_{g2})t}a^\dagger|g2\rangle\langle e|) + (e^{i\omega_h t}h(t)a^\dagger + e^{-i\omega_h t}h(t)^\dagger a)$$
$$+(e^{i(\omega_e-\omega_{g2})t}q(t)|e\rangle\langle g2| + e^{-i(\omega_e-\omega_{g2})t}q(t)^\dagger|g2\rangle\langle e|).$$

4. SUB IN FREQUENCIES

This Hamiltonian is horribly long and not fun to look at but luckily we can do some math with the frequencies to cancel some out. Going back to the diagram, we can see that ωh - ωe = -δ, ωh - ωe + ωg2 = ωg2 - δ, and ωe - ωg2 = ωq. Thus the Hamiltonian becomes

$$H = \Omega_1(e^{i\delta t}a|e\rangle\langle g1| + e^{-i\delta t}a^\dagger|g1\rangle\langle e|) + \Omega_2(e^{-i(\omega_{g2}-\delta)t}a|e\rangle\langle g2| + e^{i(\omega_{g2}-\delta)t}a^\dagger|g2\rangle\langle e|)$$
$$+(e^{i\omega_h t}h(t)a^\dagger + e^{-i\omega_h t}h(t)^\dagger a) + (e^{i\omega_q t}q(t)|e\rangle\langle g2| + e^{-i\omega_q t}q(t)^\dagger|g2\rangle\langle e|).$$

5. TAKE OUT THE TOO FAST

The final step is to take out terms with frequencies that are too fast. Note that in the interaction term between e and g2, the interaction is rotated by a frequency of ωg2 - δ. Looking at Calculating Rb Atom Frequencies, we can see that ωg2 = 6.8347GHz and since δ << 6GHz, ωg2 - δ ≈ 6.8347GHz. This rotation is way to fast for any kind of transition from e to g2 to occur so we can take the term out entirely. Note that this is a simplification and in order to be more realistic a jump term may need to be added to account for this. Adding the rotation to the drive terms so h(t) = exp(iωht)h(t) and q(t) = exp(iωqt) and replacing |gn><e| for σn gives the final Hamiltonian

$$\tilde{H} = \Omega_1(e^{i\delta t}a\sigma_1^\dagger + e^{-i\delta t}a^\dagger\sigma_1) + (h(t)a^\dagger + h(t)^\dagger a) + (q(t)\sigma_2^\dagger + q(t)^\dagger\sigma_2).$$

8. Successful Rotation of Signal-Control Simulation

[Reilly, Jeff]

I successfully simulated the Rb transition from g1 → g2 shown in the diagram below. This is for the frequency filter where the atom is only excited form g1 → e by the specific frequency we are interested in, is then brought down e → g2 by the control cavity, and finally put through the readout process in order to detect the transition.

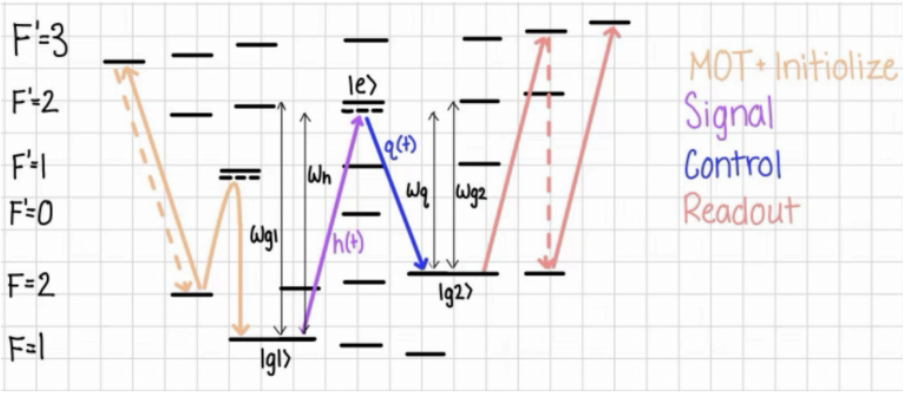

The Hamiltonian I used is based on the Jaynes-Cummings Hamiltonian but adds two drive terms, zeros the frequencies at g1, and is rotated with the cavity, excited state, and g2 state. It is of the form

$$\tilde{H} = \Omega_1(e^{i\delta t}a\sigma_1^\dagger + e^{-i\delta t}a^\dagger\sigma_1) + (h(t)a^\dagger + h(t)^\dagger a) + (q(t)\sigma_2^\dagger + q(t)^\dagger\sigma_2)$$

(look at Updated Rotating Signal-Control Hamiltonian for more info). Note that there is no interaction term between e and g2 because that frequency is spinning too fast for enough interaction to take place. h(t) and q(t) are both photons of different frequencies but for simplification they are both guassians of the form

$$h(t) = b * \exp(-\frac{(t-c)^2}{2*d^2})$$

representing the amplitude profiles in my simulation. I built a program that iterates through the width and placement of both pulses to determine what parameters result in the highest end state of g2. The optimal c and d values with set b = 5 are shown next to the graph in the diagram below. Note that both bs are set to 5 because the greater b is the greater the coupling and thus final g2

value will be so it was more valuable to iterate through both c and d values to save time.

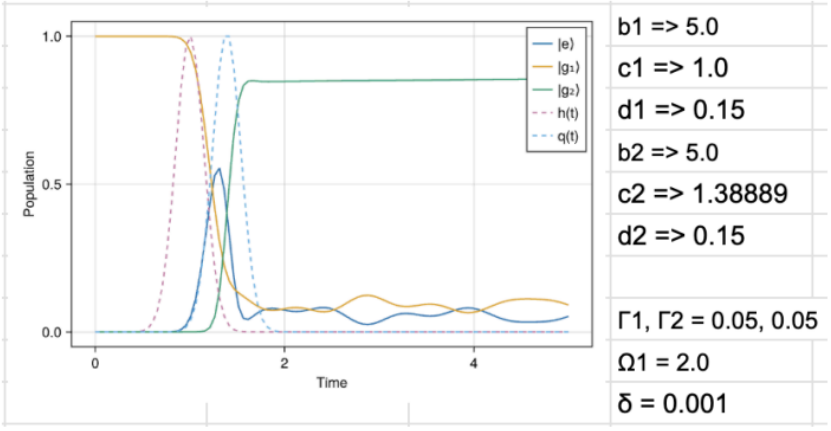

Looking at the graph, the atom starts in g1, then the photon comes in and it transitions to half g1 half e, and finally the control comes through and the atom is brought down to g2. There is still some probability in g1 and e so future work will look at decreasing that as much as possible. Note how the expectation value of g2 stays constant while e and g1 stay the same. That's because the interaction term between g1 and e remains throughout time while the coupling between g2 and e is governed by the control which goes to 0 after the pulse ends.

This final graph shows the cavity energy, the number of photons, in comparison to the atom. When the photon enters the cavity, the energy of the cavity increases. The interaction term means the energy is spread through a, g1, and e. Then when the control comes in, it couples e with g2 so some of the energy goes to g2 causing the g2 population to rise and the a, g1, and e population to decrease and thus the cavity expectation value decreases. The cavity expectation value then fluctuates with the g1 expectation value as when g1 rises that means the energy goes to the cavity and when g1 falls that means the atom has more probability in e which takes energy from the cavity causing it to fall.

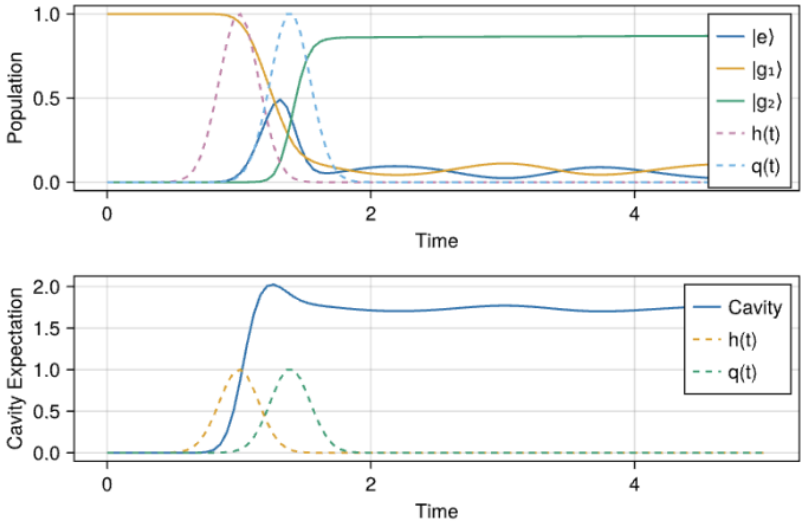

Bottom line: simulation looks good!

9. Signal and Control Photon Frequencies

[Reilly, Jeff]

I've plotted out how different frequencies of the signal and control photons effect the final g2 state. These signals are incorporated into the system via the Hamiltonian

$$\tilde{H} = \Omega_1(e^{i\delta t}a\sigma_1^\dagger + e^{-i\delta t}a^\dagger\sigma_1) + (h(t)a^\dagger + h(t)^\dagger a) + (q(t)\sigma_2^\dagger + q(t)^\dagger\sigma_2).$$

Each h(t) and q(t) equation that has a guassian (gh and gq) uses the same values as those included in Successful Rotation of Signal-Control Simulation.

FREQUENCY OF SIGNAL VS CONTROL

First I tried h(t) = gh*sin(ωh*t) and q(t) = gq*sin(ωq*t) and I got the following plot:

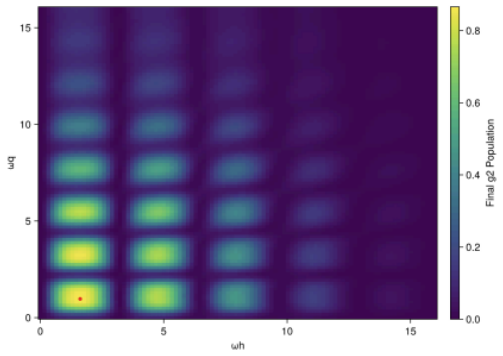

graph 1

The red dot representing the highest final g2 population has a value of 0.865635 where ωh = 1.63087 and ωq = 0.92174. This is definitely an interesting graph. I think this is because there are specific frequencies transitioning g1 → e - δ and e - δ → g2 and when ωh and ωq match these frequencies we get the greatest transition to g2. Multiples of these frequencies get some probability of the atom into the transition but less so than the pure frequency. The greater the multiple, the farther off, and the less that is transition which is why it fades as the frequencies increase.

The next shape I tried was g*exp(iωt). When rotating the Hamiltonian, both h(t) and q(t) absorbed an exp(iωht) and exp(iωqt) respectively so I wanted to see what they would look like if I put them in.

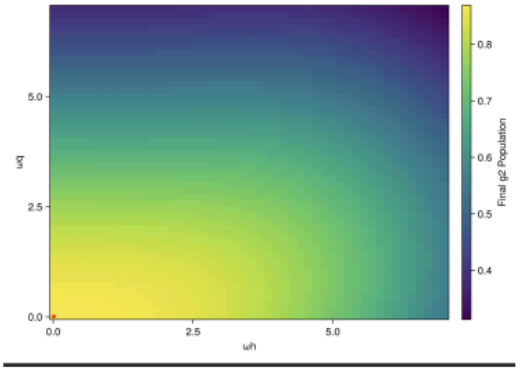

graph 2

Here the best ωh = 0.00 and ωq = 0.00 with final g2 as 0.868944. The greater the frequencies, the faster the photons are rotating. It could be that this speed deters the atom from transitioning the way we want it to.

Putting the two together, the next shape was g*sin(ωt)*exp(iωt). This graph looks almost like an overlap of the previous two graphs - the squares start to smudge out towards the edges:

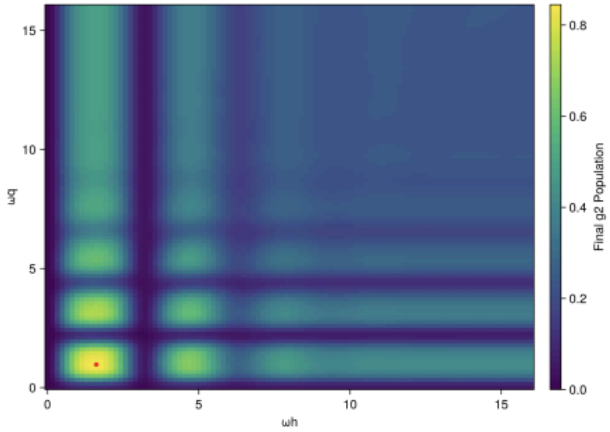

graph 3

The best ωh = 1.61616 and ωq = 0.9697 with final g2 as 0.844808. There is sort of a blur of some transition to g2 where there isn't any in the first graph because both photons are rotating so fast that some spontaneous transition occurs.

FREQUENCY DIFFERENCE VS MEAN

Next I looked at how the difference between the frequencies compared with the mean. Using the equation g*sin(ωt), we get the graph

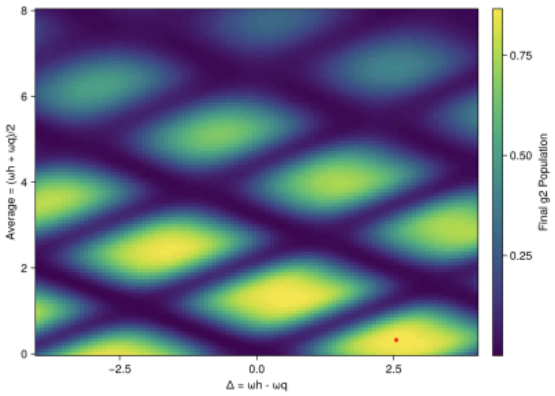

Here the best Δ = 2.54545 and avg = 0.32323 so that ωh = 1.59596 and ωq = -0.9495 with final g2 as 0.865817.

Using the equation g*sin(ωt)*exp(iωt) results in

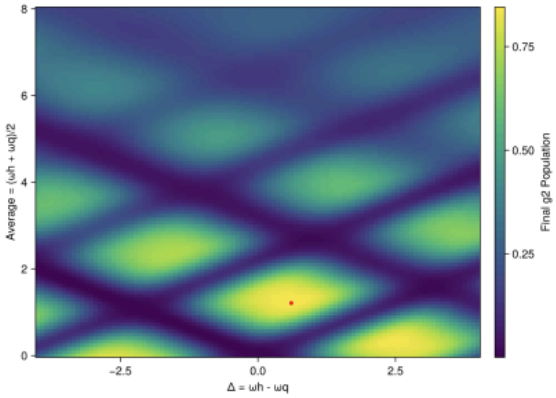

where the best Δ = 0.60606 and avg = 1.21212 thus ωh = 1.51515 and ωq = 0.90909 with final g2 as 0.845533. Interesting to note that ωh - ωq is not a constant maximum value but sort of a sinusoidal along lines with slope of about 0.5. Zooming out gives the graph

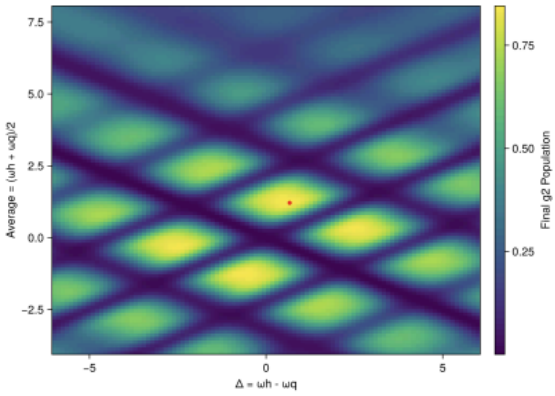

CHANGING PARAMETERS

Changing the detuning frequency δ from 0.001 → 0.00001 and 0.001 → 0.1 returns nearly the same graph as graph 3 and has the best g2 as 0.845471 where ωh = 1.61616 and ωq = 0.9697.

Increasing the placement c2 from 1.3889 → 1.5 and width d2 from 0.15 → 0.2 of the gaussian for the control has the following effect where the squares of the control frequency are sort of split in half. The best frequencies are ωh = 1.45455 and ωq = 0.48485 with final g2 as 0.821403.

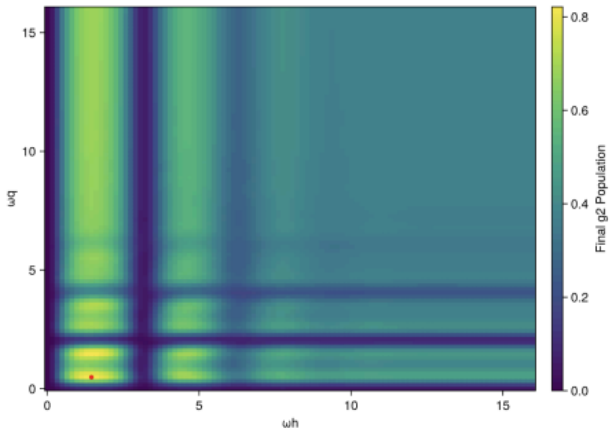

Decreasing the placement c1 from 1.0 → 0.5 and width d1 0.15 → 0.1 of the signal photon guassian elongates the squares along the x direction and rendering the following graph. Here the best frequencies are ωh = 2.58586 and ωq = 1.61616 with final g2 as 0.405857.

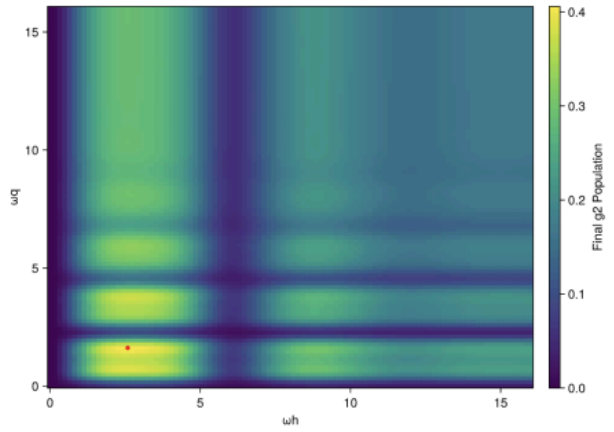

CONCLUSION

When ωh = the transition frequency from g1 → e-δ and ωq = the transition from e-δ → g2 there is a maximum transition to g2 denoted by the red dot. The graphs below show one frequency staying constant at it's optimal value and just looking at how changing the other frequency changes the g2 population. There are lines of maximum g2 population at the optimal transition frequency and then other lines of lower maximums at multiples of the frequency.

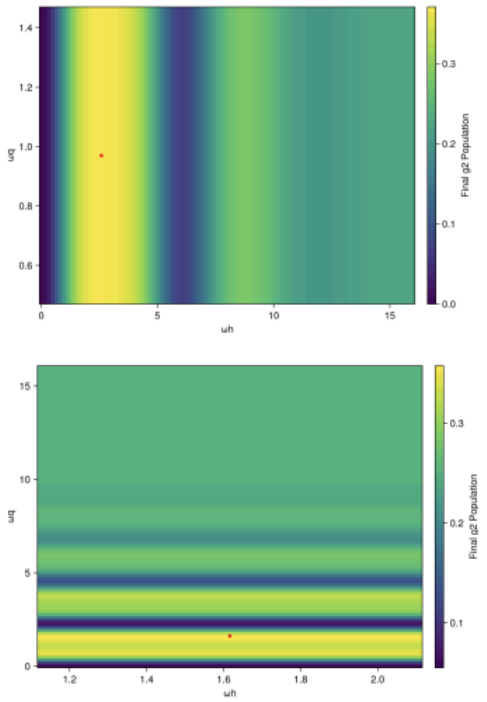

It's clear that these patterns overlap to cause the squares. There is also a lot of fading when the frequencies are increased due to the exp(iωt) term causing some spontaneous transitions.

Changing the gaussian and thus the amplitude profile will change how these frequency maximums look.

10. Optimizing Control Parameters

[Reilly, Jeff]

I created a new file that goes through the various parameters of the control photon to try and maximize the final g2 expectation value.

SETUP

The system is set up as a 3-level Λ-type atom replicating the signal-control transition of the Rb atom in the cavity. The Hamiltonian of the system is rotated in the cavity, excited state, and g2 state where the energy of g1 is set at 0. It's of the form

$$H = H_{\text{int}} + H_{\text{sig}}(t) + H_{\text{control}}(t)$$

where

$$\begin{aligned} H_{\text{int}} &= \Omega_1(e^{i\delta t}\sigma_1 a^\dagger + e^{-i\delta t}\sigma_1^\dagger a), \\ H_{\text{sig}}(t) &= h(t)^\dagger a + h(t)a^\dagger, \\ H_{\text{cont}}(t) &= q(t)^\dagger \sigma_2 + q(t)\sigma_2^\dagger. \end{aligned}$$

Both h(t) and q(t) are of the form g*sin(ωt)*exp(iωt) where g is a gaussian such that

$$g = b * \exp(-\frac{(t-c)^2}{2*d^2}).$$

Thus b corresponds to the height of the pulse, c to the timing, and d to the width. This system also has collapse operators

$$\text{collapse} = [\sqrt{\Gamma 1} * \sigma 1, \sqrt{\Gamma 2} * \sigma 2, \sqrt{\Gamma 3} * a]$$

where σ1 = |e>→|g1>, σ2 = |e>→|g2>, and a is the cavity annihilation operator and `Γ1, Γ2, Γ3 = 0.05, 0.05, 0.005`. Finally, note that the detuning frequency δ = 0.001 and ωh = 1.1 - these frequencies are not an accurate representation of the Rb system but I'm using them for now as they are easier to run calculations with and the ratio of ωh/δ is similar to the actual ratio. The guassian for the signal photon is described in optimal parameters in the figure below.

SIMULATIONS

Running through each parameter of the control photon gaussian and frequency results in the following graphs. The final population vs time graph uses the optimal parameters found in the initial graphs and looks at the population of each state over time.

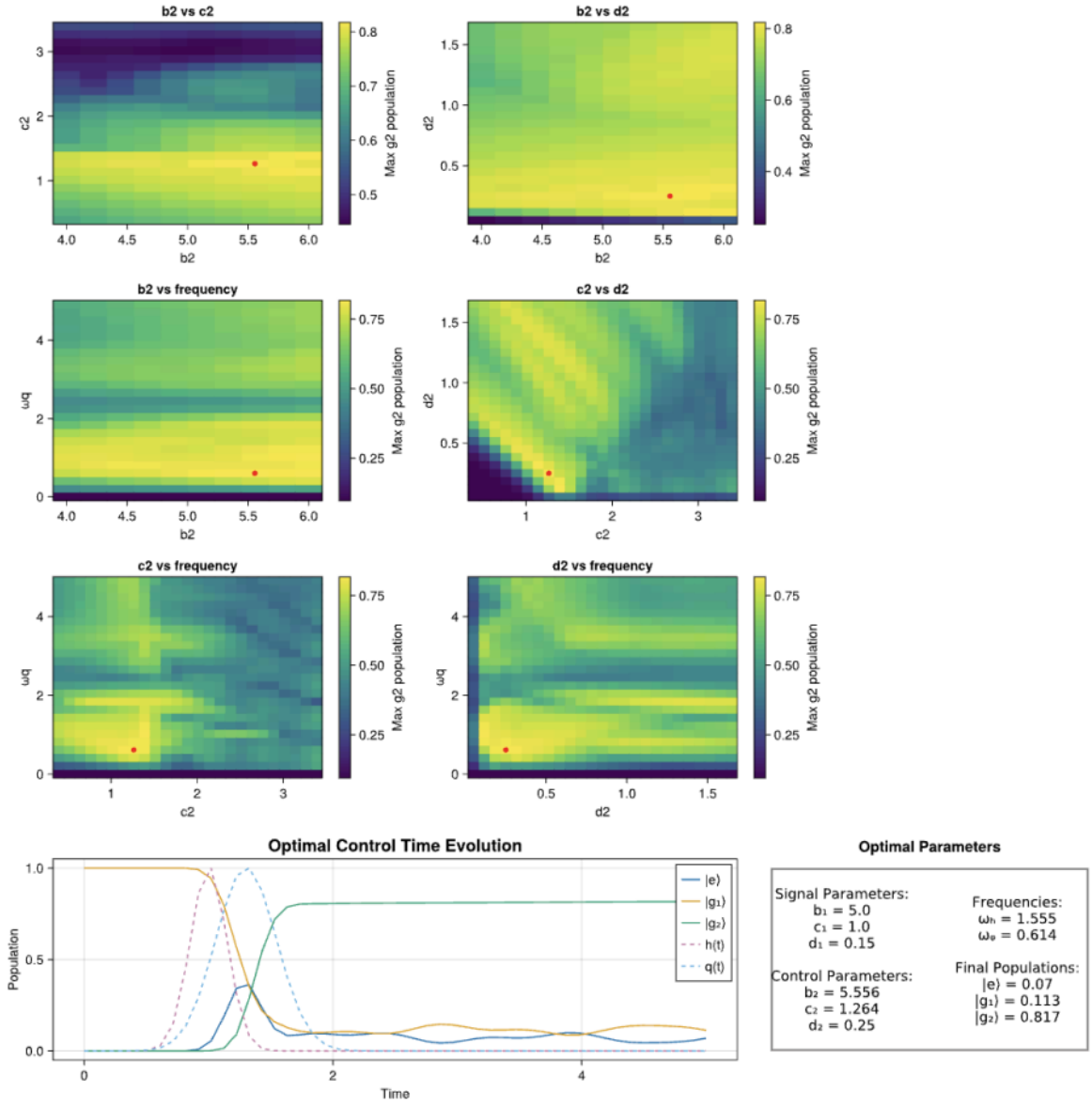

Note that the graphs are a little grainy - iterating through four different parameters takes some time so i only went through 20 different values for each but could go farther later. Each graph with ωq has a similar pattern as that found in the Signal and Control Photon Frequencies where there's a peak that goes down on either side and then comes back up along the axis. The c2 vs d2 graph is also interesting as it's the only one with a diagonal pattern instead of a horizontal one. As the timing of the pulse increases, the width decreases - it's interesting to think about why this may be as you'd think the opposite would happen to keep the start of the pulse in place. The b2 vs c2 graph has a drop off after a c2 = 2.5 which is probably when the control photon hits where g1 has fluctuated back up and e has gone back down and thus no population can transfer to g2. Finally, the b2 vs d2 graph shows not much of a correlation. I'm not entirely sure why this is nor why it seems to dip near d2 = 1.25 and b2 = 4.

CONCLUSIONS

Interesting to see how the various parameters of the control photon relate to each other. Would also be fun to make a program that goes through the signal photon values too and takes precise steps to really maximize the final g2 value. Also could be interesting to calculate QFI for each parameter to see the dependence of the final state.

11. Time Reversal and Wigner Function1

[Reilly, Jeff]

The system here is shown in the diagram below:

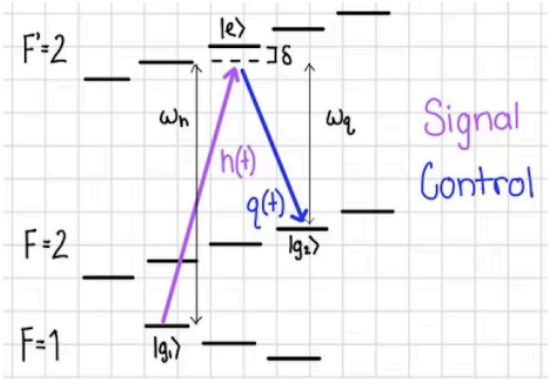

This is where the signal from the interferometers enters the cavity. The signal excites the atom up from g1 → e and then a control pulse brings the atom from e → g2. We design the control pulse such that only signal photons with the specific shape that we are looking for will excite the atom to this effective two level system. In a previous lab log I looked at optimizing the control pulse based on the signal pulse and now wanted to see if I time reversed the process if I could get the same signal photon out of the system. Starting in the g2 state (not entirely g2 - I used the end populations when simulating the forward system which was mostly g2 but still a little in the other states) and sending the control pulse sends the atom up to the detuned e state and then when it decays down to g1, the atom should release a photon that looks the same as the signal photon that I optimized the control on. Simulating this process results in the graphs below.

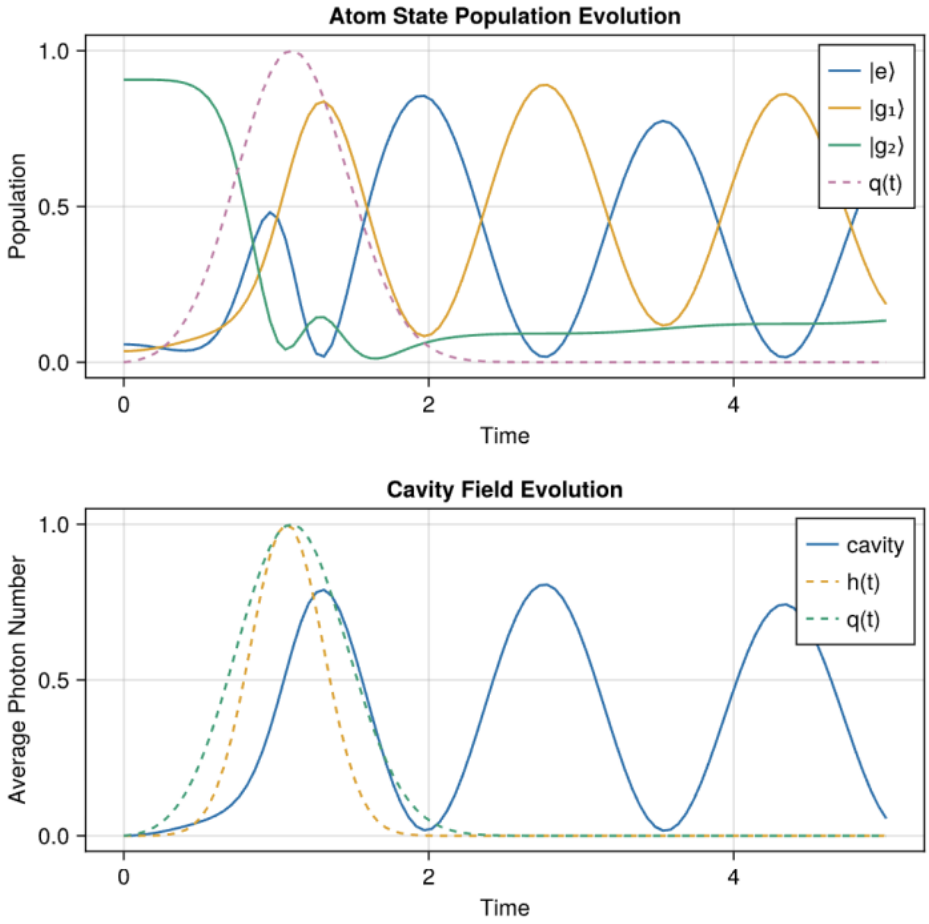

Looking at the first graph, you can see how the control pulse causes coupling between e and g2 and ends with g2 near zero. Then e and g1 are coupled through the interaction term in the Hamiltonian. G2 steadily rises due to the spontaneous decay of e → g2. Looking at the second graph, you can see how the cavity changes as well as the control pulse and what I would expect the signal pulse to look like. The expected signal pulse is the same shape as the signal pulse the control pulse was optimized from but it's moved positively in time by the same difference as the original signal and control pulse. The photon released here is similar in shape - the amplitude of the signal pulse is actually up to 5 and is normalized to fit on the graph.

12. QFI Per Parameter

[Reilly, Jeff]

I thought it'd be interesting to look at the QFI over time for each of the parameters of the signal and control photons driving Rb atom transitions in cavity. This system has the following system:

$$H = \Omega_1(e^{i\delta t}\sigma_1 a^\dagger + e^{-i\delta t}\sigma_1^\dagger a) + h(t)^\dagger a + h(t)a^\dagger + q(t)^\dagger\sigma_2 + q(t)\sigma_2^\dagger$$

where

$$h(t) = (b_1 * \exp(-\frac{(t-c_1)^2}{2*d_1^2}) * \sin(\omega_h t) * \exp(i\omega_h t)$$

and

$$q(t) = (b_2 * \exp(-\frac{(t-c_2)^2}{2*d_2^2}) * \sin(\omega_q t) * \exp(i\omega_q t)$$

and collapse opperator $L = [\sqrt{\Gamma 1} * \sigma_1, \sqrt{\Gamma 2} * \sigma_2, \sqrt{\Gamma 3} * a]$.

(δ = detuning frequency; Ω1 = coupling strength btwn g1 → e; σn = |e><gn|; Γ1, Γ2 ,Γ3 = decay rates of e→g1, e→g2, e→cavity). Each parameter is set with the value shown in the upper right corner of the graph. The time evolution of the system is shown in the first plot and the QFI for each operator over time is shown after (you can specify which parameters you'd like to look at in the simulation but figured I'd show all of them here)

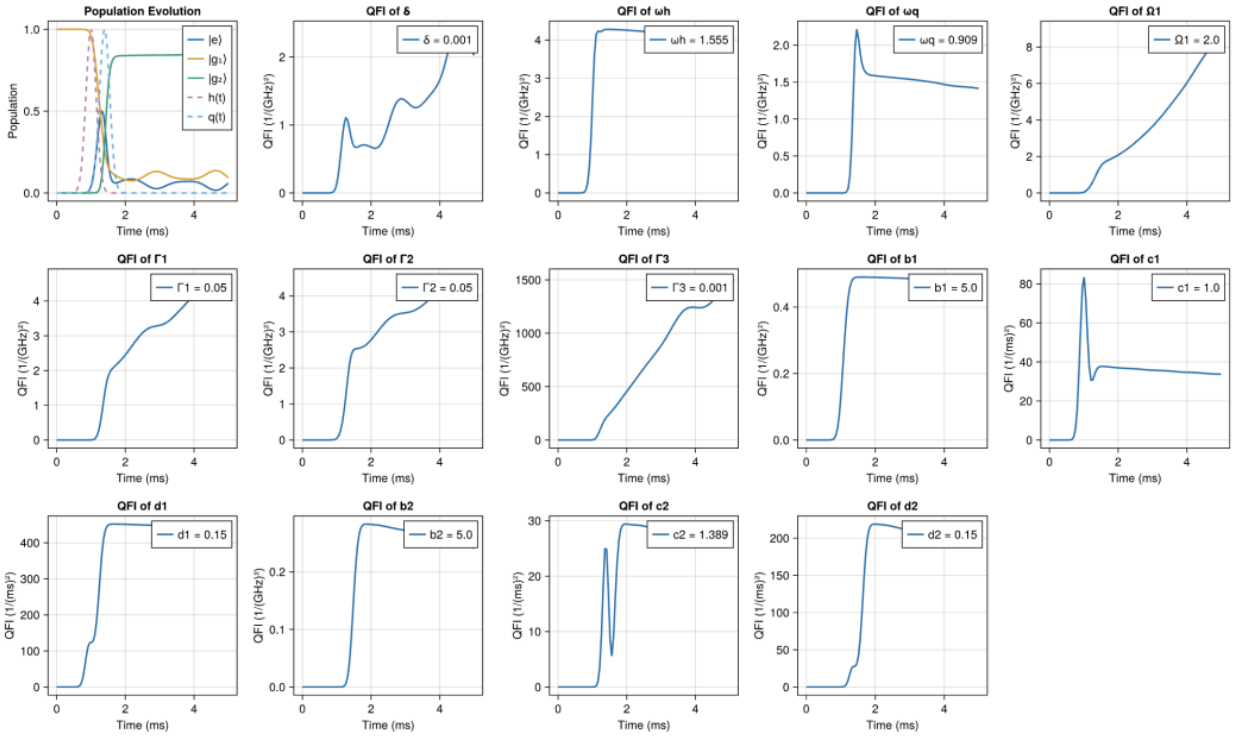

Things to note:

- detuning δ: QFI has a max where |e> has a max - makes sense cause when detuning changes the probability of g1 → e will change cause drive will be off resonance. later QFI increases and sort of fluctuates with \e>
- drive frequencies ωh and ωq: both have maxes where their corresponding photons have maxes cause changes in drive frequency will change where g1 and e go and thus the amount of the population that is transferd from the state. Interesting that ωq dips after the max but ωh stays flatter - you'd think they'd have the same shape as they are sort of doing the same thing just with different transitions. Also note how ωq QFI is about half that of ωh.
- coupling strength Ω1: steady increase over time
- decay rates Γ1-3: constantly increasing over time. note how Γ1 and 2 (corresponding to decay rates of e→g1 and 2) have a steeper slope where the corresponding transition occurs - likely due to how there can be no decay from e until there is population there and once there is it starts decaying it does so at the given rate. Also note how much greater the Γ3 QFI is - likely due to how energy is then leaving the atom into the cavity which can't be recovered back into the atom.
- photon amplitudes b1, b2: both have similar shapes and peak at the time of the photon's arrival but note the of b1 is consistently about 2x b2
- photon positions c1, c2: both have peaks at about the time of their value but note that c1's peak is about 3x c2's peak. Afterwards, both settle to similar values.
- photon widths d1, d2: once again both have similar shapes that peak at the time of their respective photons but the QFI of d1 is 2x that of d2. Also note both have a little bump during the incline to the peak likely due to the changing start time of the photon.

Conclusion: The end state value is much more sensitive to the parameters of the signal photon than the control photon. Changing the parameters of the photon tends to have a constant QFI after the photons are absorbed where as the atomic and cavity parameters have increasing QFIs over time.